Komkris Boonying[1], Chuwong Phongcharoenpanich[2]

Faculty of Engineering, Rajamangala University of Technology Rattanakosin, Nakhon Pathom (1), Thailand
Faculty of Engineering, King Mongkut's Institute of Technology Ladkrabang (2), Thailand

doi:10.15199/48.2020.01.23

Analysis and Design of Circularly Polarized Capacitively-Fed Planar Suspended Antenna for Universal UHF RFID Applications

Abstract. *This research paper deals with the design of a circularly polarized reader antenna with a tennis ball-shaped radiating plate that operates at a frequency range of 860-960 MHz with the center frequency of 910 MHz. In the fabrication of the tennis ball-shaped radiating plate, a small annular-ring slot was first created on a circular radiating plate, followed by two diagonally opposite large arc-shaped annular-ring slots on either edge of the circular radiating plate and then the truncation of the corners of the remaining main element of the plate. A prototype antenna with the final tennis ball-shaped plate was subsequently assembled prior to excitation by the capacitively coupled feed technique to enhance $|S_{11}|$ bandwidth. The prototype antenna could achieve an average gain of 6.18 dBic, $|S_{11}|$ covering the frequency range of 837.6-966.2 MHz, and the circular polarization of 850.6-963.5 MHz, making it suitable for universal UHF RFID applications. In addition, simulations were carried out using CST Microwave Studio for comparison with the experimental results.*

Streszczenie. *W artykule zaprezentowano projekt anteny o kształcie piłki tenisowej pracujacej w zakresie częstotliwopści 860 – 960 MHz. Prototyp anteny pokrywał zakrs 837.6 – 966.2 MHz co spełnia wymagania uniwersalnej komunikacji UHF RFID.* ***Projekt i analiza planarnej anteny cyrkularnie polaryzowanej do zastosowań w UHF RFID transmisji danych***

Keywords: Capacitively coupled feed, circular polarization, suspended structure, truncation corners, UHF RFID.
Słowa kluczowe: antena RFID, antena cyrkularnie polaryzowana, antena planarna

Introduction

Based on the radar principle, radio frequency identification (RFID) technology is suitable for objects identification and tracking applications. In a typical RFID system which consists of a tag and a reader antenna, the exchange of data is carried out through electromagnetic waves. Currently, the RFID technology has found its usefulness in manufacturing, security, logistics and transportation [1-2]. Of the existing RFID bands, the Ultra High Frequency (UHF) RFID band is commonly adopted for various applications due to its long readable range, higher transfer rate and robust capability. According to the International Standardization Organization (ISO)'s 18000-63 standard, the UHF RFID universal band refers to the frequency range of 860-960 MHz [3]. The Europe Union (EU) and the city-state of Singapore have adopted the 866-869 MHz frequency. The Americas and some Asian nations have used 902-928 MHz, while Japan and several other Asian countries have implemented 952-955 MHz. Typically, the design of the tag is of dipole antenna with a linearly polarized (LP) radiation, and so is the design of the reader antenna with the linearly polarized radiation. Nevertheless, due to the inherent multipath fading and mismatch polarization of the tag (when rotated positions), the design of reader antenna of this research is of circularly polarized (CP) radiation to overcome both issues.

Previous research [4-14] investigated three existing UHF RFID reader antenna structures fed by single linear electric coaxial probe: the single-layer, suspended, and stacked antennas. The first structure (i.e. the single-layer antennas) could achieve the less satisfactory $|S_{11}|$ bandwidth (BW) of 1-2% and gain of <4 dBi, but the advantages of this structure are its low profile and ease of fabrication [4-6]. The suspended structure (with an air gap) could achieve a better $|S_{11}|$ BW of 4-5% and a higher gain of <9 dBi [7-12]. With the stacked structure antenna (multi-layer structure), the $|S_{11}|$ BW was enhanced to >10% with a much higher gain of >9 dBi [4, 7, 13-14]; however, it is bulky and difficult to design.

In [15-25], the previously three structures were experimented with different feeding methods to improve the $|S_{11}|$ BW. The stacked [15] and suspended structured antennas [16] with an L-shaped feeding probe could achieve the $|S_{11}|$ BW of >22%. The suspended [17] and single structured antennas [18] with an F-shaped feeding probe produced the $|S_{11}|$ BW of >15%. In [19], the suspended structure antenna with a T-shaped feeding probe achieved the $|S_{11}|$ BW of 41% with an SWR of <2. The stacked structured antenna with an aperture couple feeding achieved the $|S_{11}|$ BW of >25% [20-21]. In [22], the stacked structured antenna with strip or line plate feeding connected directly to the radiating plate could achieve the $|S_{11}|$ BW of >25.8%. In [23-24], the suspended structured antenna with capacitively coupled feeding on the same plane as but outside the radiating plate produced the $|S_{11}|$ BW of >25%. The suspended antenna with capacitive feed (i.e. rectangular slot near the feeding probe) on the radiating plate generated the $|S_{11}|$ BW of 5.3% [25].

In addition, various CP-radiation generating techniques were employed in [26-32]. In [4-7, 26], the truncation technique whereby the corners or edges of the radiating plate are truncated were discussed. The insertion technique with slot, slit, strip plate or spur line on the radiating plate or at the corners or edges of the plate were experimented in [4-7, 18, 26-30]. In addition, the generation of CP radiation was achieved with the use of cross or orthogonal antennas [4-7, 31]. In [4, 7, 32], an antenna with square radiating plate was integrated with a Wilkinson power divider circuit with 90° phase difference.

This research paper has proposed a square suspended-structure antenna with tennis ball-shaped radiating plate excited by the capacitively coupled feed technique to fully cover the universal UHF RFID band. In the fabrication of the tennis ball-shaped plate, a small annular-ring slot was first created on a circular radiating plate, followed by two diagonally opposite large arc-shaped annular-ring slots on either edge of the circular radiating plate and the truncation of the corners of the main section of the radiating plate. In the implementation of the capacitively coupled feeding technique, a small annular-ring slot was connected to a coaxial probe to enhance and achieve the $|S_{11}|$ BW of 14.13% (837.6-966.2 MHz). A paring and the truncation techniques of the CP radiation were achieved a 3-dB axial ratio (AR) BW of 12.41% (850.6-963.5 MHz) with the average gain within the universal UHF RFID band of 6.18 dBic.

The organization of the rest of the paper is as follows: Section II details the structure, evolution and design of the proposed antenna. Section III discusses the parametric study of the initial antenna, capacitively coupled feed, paring and truncation techniques. Section IV deals with the simulation and measurement results with regard to the $|S_{11}|$ BW, AR BW, radiation patterns and gains. The simulations were carried out using the CST MICROWAVE STUDIO software program. The concluding remarks are provided in Section V.

Antenna structure and design

Figure 1 illustrates the geometry of the proposed UHF RFID reader antenna. The antenna was composed of a 165 × 165 mm square-shaped structure (G) and the tennis ball-shaped radiating plate of 69.7 mm in radius (R). The height (h_d) of the epoxy substrate (ε_r=3.78) was 1.6 mm, while the copper thickness (t_p) and loss tangent of the substrate were 0.03 mm and 0.04, respectively. The antenna design was of suspended structure with a 42 mm air-gap (h_a) between the radiating plate and the ground plane. In addition, on the radiating plate was a small annular-ring slot which was directly connected to a linear electric coaxial probe

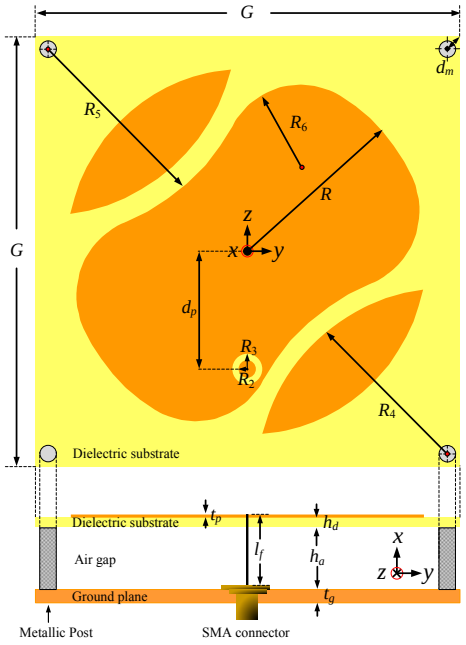

Fig.1. Geometry of the UHF RFID reader antenna

The capacitively coupled feed (i.e. the small annular-ring slot) was located vertically opposite to the center of the radiating plate with a distance point (d_p) of 45 mm. The inner (R_2) and outer (R_3) radii of the small annular-ring slot were 3.17 mm and 5.6 mm, respectively. The feeding probe length (l_f) and the ground plane thickness (t_g) were respectively 43.6 mm and 1.6 mm. Four metallic posts were mounted between the radiating plate and the ground plane and the distance (d_m) from the metallic post center to its nearest antenna corner was 7.07 mm. Two of the metallic post centers of opposite corners served as the center points from which two large arc-shaped annular-ring slots were created. The double paring divided the circular radiating plate into three sections, consisting of two leaf-shaped sections and one large middle section. The inner (R_4) and outer (R_5) radii of the large annular-ring slots were 74 and 81.5 mm, respectively. The four corners of the middle section of the radiating plate were subsequently truncated into arc shape with a radius (R_6) of 30 mm individually. The amalgamation of the three sections (i.e. two leaf-shaped sections and the middle section) formed the tennis ball-shaped radiating plate of the proposed antenna.

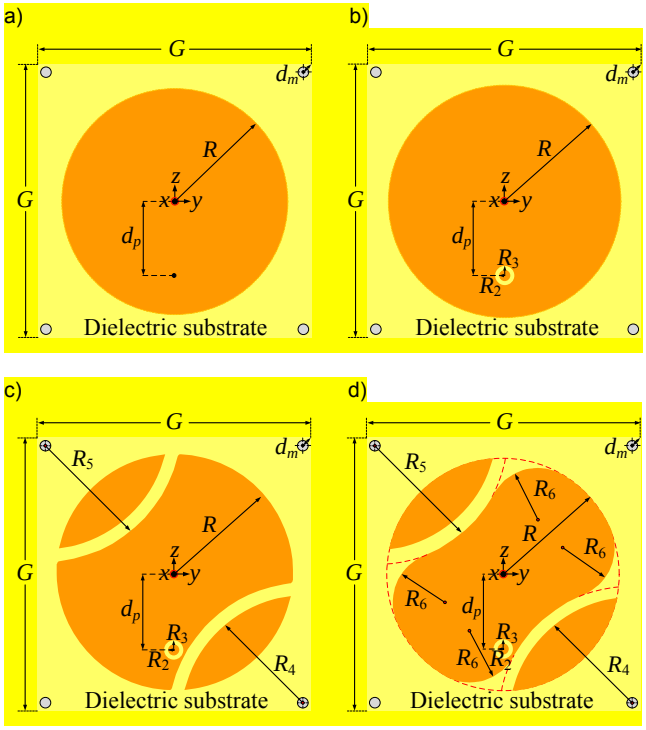

Fig. 2. Design evolution of the proposed antenna: (a) circular radiating plate antenna (stage#1), (b) the antenna with a small annular-ring slot (stage#2), (c) generation of two large annular-ring slots (stage#3), (d) truncation of four corners (stage#4 or proposed antenna).

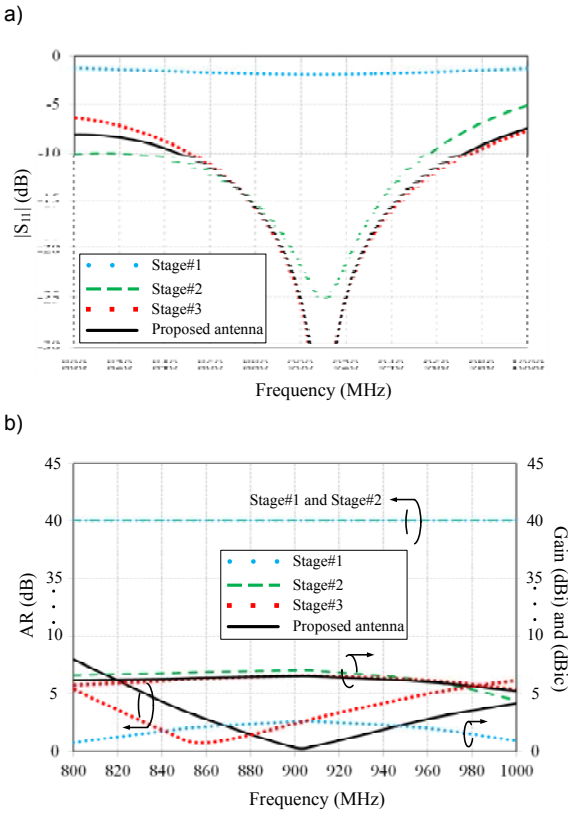

Fig. 3. Comparison of the simulated $|S_{11}|$, AR and gain for the four stages of the antenna evolution (a) $|S_{11}|$, (b) AR and rad gain.

Table 1. The parametric values at the four stages of the antenna evolution

Parameters	Stage#1 (mm.)	Stage#2 (mm.)	Stage#3 (mm.)	Proposed antenna (mm.)
G	165	165	165	165
h_a	42	42	42	42
h_d	1.6	1.6	1.6	1.6
d_p	45	45	45	45
d_m	7.07	7.07	7.07	7.07
R	63.23	69.7	69.7	69.7
R_2	-	3.45	3	3.17
R_3	-	6.4	5.6	5.6
R_4	-	-	74	74
R_5	-	-	81.5	81.5
R_6	-	-	-	30

Figure 2 illustrates the design evolution of the proposed antenna, consisting of four main stages. Fig. 2 (a) depicts the initial suspended-structure antenna excited with linear electric coaxial probe (stage#1). In stage#2, to enhance the $|S_{11}|$ BW, the capacitively coupled feeding technique using the small annular-ring slot as the feeding point was implemented, as shown in Fig. 2 (b). In stage#3, the two large arc-shaped annular-ring slots (i.e. two leaf-shaped sections) were created for generation of the CP radiation (Fig. 2 (c)). The remaining middle section of the radiating plate was subsequently truncated along its four corners to shift the AR to approach the center frequency. The three sections in combination produced the tennis ball-shaped radiating plate of the proposed antenna (stage#4), as shown in Fig. 2 (d). Table 1 presents the parametric values at the four stages of the evolution of the proposed antenna.

Figure 3 (a) illustrates the simulated $|S_{11}|$ BW throughout the evolution of the proposed antenna. At the first stage of the evolution, an impedance mismatch was observed. With the introduction of the small annular-ring slot (stage#2), the $|S_{11}|$ BW of 15.69% (814.2-957 MHz) was achieved. In stage#3, the $|S_{11}|$ BW was 13.71% (850.8-975.6 MHz), and the proposed antenna (stage#4) could achieve the $|S_{11}|$ BW of 13.89% (845.8-972.2 MHz).

Figure 3 (b) shows the simulated 3-dB AR BW and gains throughout the antenna evolution. Both stages#1 and #2 could achieve the simulated AR BWs of 40.00 dB with 21.98% (800-1000 MHz) and were of linearly polarized radiation. The 3-dB AR BW achieved in stage#3 at the resonant frequency of 860 MHz was 9.88% (827.5-912.5 MHz), while that of stage#4 (the proposed antenna) at the center frequency (910 MHz) was 12.31% (853-965 MHz). The average simulated gains for stages#1 and #2 of the antenna evolution were <3 and >6 dBi, while those for stages#3 and #4 were >6 dBic.

Parametric study

This section discusses the suspended-structure initial antenna, the capacitively coupled feed technique for the $|S_{11}|$ BW enhancement, the paring technique to create the two arc-shaped large annular-ring slots for CP radiation generation, and the corners-truncation technique for shifting the AR to be near the center frequency. The proposed reader antenna is developed for use in the UHF RFID system and applications. The $|S_{11}|$, $|S_{11}|$ BW, 3-dB AR BW and gain are the deciding criteria for the suitability and applicability of the antenna.

Initial antenna at stage#1, the radius of the circular radiating plate of the suspended-structure initial antenna was determined using TM_{110} mode [16, 33]. The basic design parameters of the initial suspended antenna encompass the height of the air-gap (h_a), the height of the dielectric substrate (h_d) and the dielectric constant (ε_r) were 42 mm, 1.6 mm and 3.78, respectively. Based on [16, 33], the resultant radius of the circular radiating plate at the center frequency (910 MHz) was 59.23 mm. Nonetheless, the air-gap height of a typical suspended-structure antenna with linear electric coaxial probe is limited to not exceeding 20 mm; otherwise, the impedance mismatch would ensue. To overcome the height limitation, the capacitively coupled feeding technique was integrated with the linear coaxial feed for impedance matching and the $|S_{11}|$ BW enhancement. Figure 4 depicts the simulated $|S_{11}|$ and resonant frequencies achieved with five circular radiating plate radii (R) of 55.23, 59.23, 63.23, 67.23 and 71.23 mm. The resonant frequencies for the radii of 55.23, 59.23 (identical to the above calculation), 63.23, 67.23 and 71.23 mm were 1000, 960, 910, 870 and 825 MHz, respectively, with varied impedance mismatch. At this stage, the simulated gain was <3.00 dBi and the radiation was purely linear polarization with AR of 40 dB, as shown in Fig.3 (b).

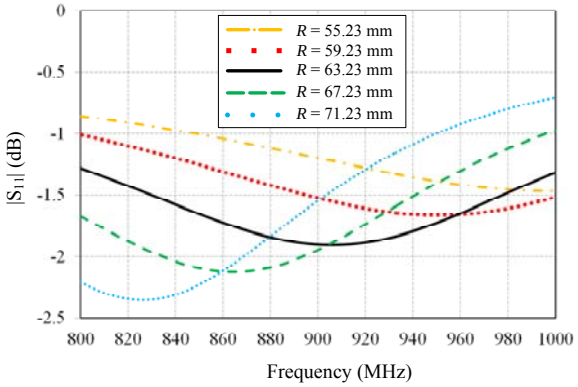

Fig. 4. The simulated $|S_{11}|$ relative to resonant frequency for various radii (R) of the circular radiating plate (stage#1).

a)

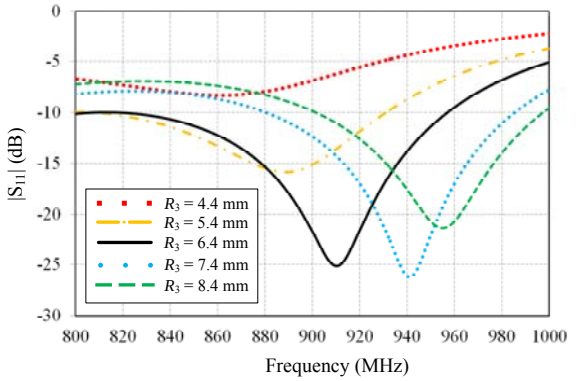

b)

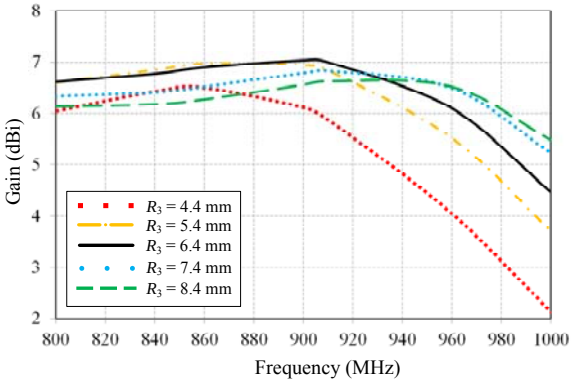

Fig. 5. The simulation results by varying R_3 (stage#2): (a) $|S_{11}|$ versus frequency (b) gains versus frequency.

Capacitively coupled feed technique (stage#2). At stage#2, the capacitively coupled feeding technique was employed to matching and enhancing the $|S_{11}|$ BW (Fig. 5 (a)). In general, the insertion of slots into the radiating plate of an antenna affects the resonant frequency of the antenna. In this research, the radius (R) of the circular radiating plate thus required optimization and the optimal R was 69.7 mm with the resonant frequency of 910 MHz (i.e. the center frequency). At this stage, the simulations were carried out by varying the outer radius of the small annular-ring slot R_3 (i.e. 4.4, 5.4, 6.4, 7.4, 8.4 mm) while using G, h_a, h_d, d_p, d_m, R and R_2 from Table 1. Similar to those of stage#1, the polarization and beam achieved in stage#2 were vertical and unidirectional, respectively. Figure 5 (a) illustrates the simulated $|S_{11}|$ and $|S_{11}|$ BW for the various outer radii of the small annular-ring slot R_3. The simulated resonant frequencies and $|S_{11}|$ BWs for R_3 of 4.4, 5.4, 6.4, 7.4 and 8.4 mm, respectively, were 865 MHz (with impedance mismatch and no $|S_{11}|$ BW), 890 MHz (BW of 12.96%), 910 MHz (15.69%), 940 MHz (11.58%) and 953 MHz (10.63%). The R_3 of 6.4 mm was resonant center frequency and $|S_{11}|$ BW of 814.2-957 MHz (15.69%) indicated the failure to cover the universal UHF RFID band. In Figure 5 (b), the maximum gain of 7.12 dBi at the center frequency (910 MHz) was achieved for R_3 of 6.4 mm, while the average gains achieved with R_3 of 5.4, 6.4, 7.4 and 8.4 mm were >6.50 dBi, except for the case of R_3 = 4.4 mm where there was impedance mismatch was average gain of 5.63 dBi.

Paring technique (stage#3). In the third stage, the simulations were carried out to identify R_4 that provided the lowest AR by concurrently varying the inner radii (R_4) of the two large annular-ring slots. In this research, the maximum outer radius (R_5) of the large annular-ring slots was limited to 81.5 mm to avoid an overlap with the small annular-ring slot. In addition, except for R_4 which was varied between 44-80 mm, G, h_a, h_d, d_p, d_m, R, R_2, R_3 and R_5 were referred to the optimal values in Table 1. Figure 6 (a) illustrates the simulated $|S_{11}|$ and $|S_{11}|$ BW relative to the resonant frequency for varying R_4 (i.e. 44, 50, 56, 62, 68, 74 and 80 mm). The simulated resonant frequencies for R_4 of 44 (without two leaf-shaped sections), 50 (with two "smallest" leaf-shaped sections and "widest" gap between the leaf-shaped and middle sections), 56, 62, 68, 74 and 80 mm (with two "largest" leaf-shaped sections and "narrowest" gap between the leaf-shaped and middle sections), respectively, were 903.8 (BW of 11.65%), 893.4 (11.69%), 903.81 (11.67%), 904.4 (11.71%), 905.4 (12.70%), 910 (13.71%) and 913.6 MHz (14.95%). The simulation results also showed that, except for that of 50 mm, R_4 of 44 mm and 56-80 mm generated the frequencies that covered the universal UHF RFID band (860-960 MHz). The frequency range for R_4 of 50 mm was 844.4-951.6 MHz. Figure 6 (b) illustrates the simulated AR relative to the resonant frequency for the various R_4. The simulated 3-dB AR BW for R_4 of 44 (without two leaf-shaped sections), 50 (with two "smallest" leaf-shaped sections and "widest" gap between the leaf-shaped and middle sections), 56, 62, 68, 74 and 80 mm (with two "largest" leaf-shaped sections and "narrowest" gap between the leaf-shaped and middle sections), respectively, were 9.01%, 9.83%, 9.24%, 9.3%, 9.77% at 860 MHz and 9.88% at 843.3 MHz. Based on the simulation results, an AR of <0.8 dB could be achieved only for R_4 of 74 mm. In addition, the simulated 3-dB AR BW for all the R_4 (i.e. 44–80 mm) indicated the failure to cover the universal UHF RFID band. Figure 6 (c) depicts the simulated gains for the various R_4. The average gain was >6.15 dBic (860-960 MHz) with the highest gain of >6.25 dBic achieved at R_4 of 80 mm. (with two "largest" leaf-shaped sections and "narrowest" gap between the leaf-shaped and middle sections).

Truncation technique (stage#4). In the final stage, the four corners of the middle section of the radiating plate were truncated into arc shape with a radius (R_6) of 20-35 mm to shift the AR in order to reach the center frequency. The amalgamation of the two small leaf-shaped and the large middle sections subsequently formed the tennis ball-shaped radiating plate of the proposed antenna. At stage#4, R_6 was varied between 20 and 35 mm, while G, h_a, h_d, d_p, d_m, R, R_2, R_3, R_4 and R_5 were referred to the optimal values in Table 1. Figure 7 (a) illustrates the simulated $|S_{11}|$ and $|S_{11}|$ BW relative to the resonant frequency for varying R_6 (i.e. 20, 25, 30 and 35 mm). The simulated resonant frequencies for R_6 of 20, 25, 30 and 35 mm were 896.6 MHz (BW of 13.45%), 916.8 MHz (13.51%), 910 MHz (13.89%) and 910.4 MHz (14.46%), respectively.

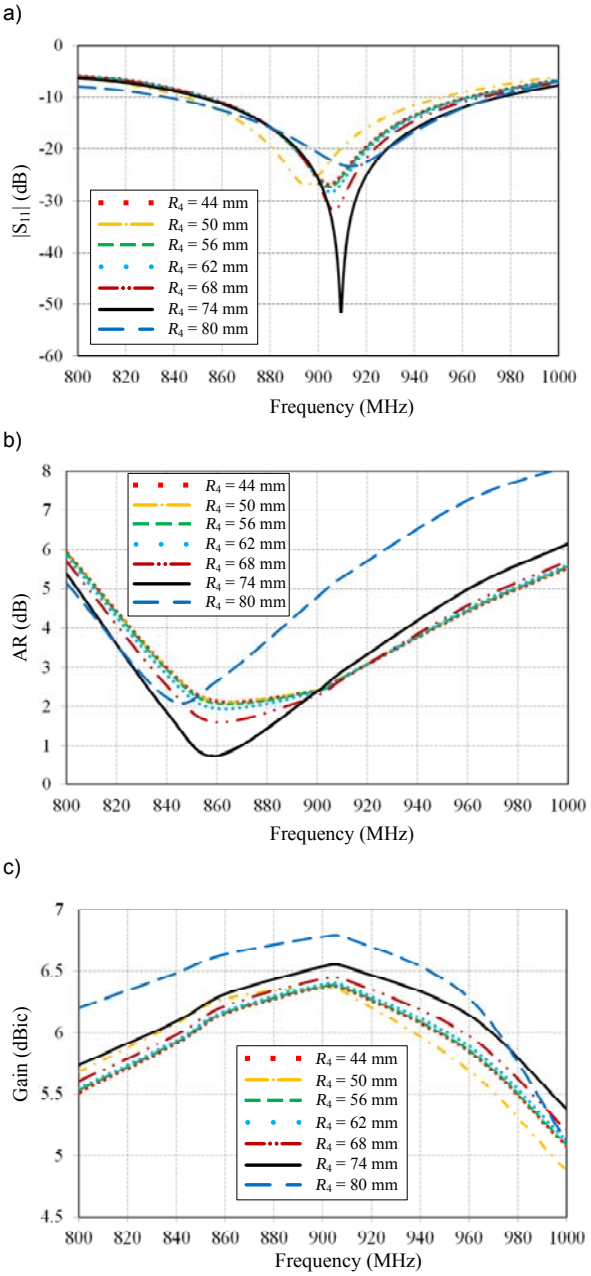

Fig. 6. The simulation results by varying R_4 (stage#3): (a) $|S_{11}|$, (b) AR and (c) gain.

The simulated $|S_{11}|$ BW for all the R_6 (i.e. 20–35 mm) indicated to cover the universal UHF RFID band.

Figure 7 (b) shows the simulated 3-dB AR BW relative to frequency for the various R_6. The simulated 3-dB AR BW for R_6 of 20, 25, 30 and 35 mm, respectively, were 11.2% of BW (838.1-940 MHz), 11.26% (847.5-950 MHz), 12.31% (853-965 MHz) and 12.7% (871.9-987.5 MHz). The findings also revealed that it was only R_6 of 30 mm that the simulated 3-dB AR BW covered the universal UHF RFID band. Figure 7 (c) depicts the simulated gains for the various R_6. The maximum simulated gains for R_6 of 20, 25, 30 and 35 mm, respectively, were 6.52 dBic at 900 MHz, 6.48 dBic at 910 MHz, 6.50 dBic at 900 MHz, and 6.5 dBic at 900 MHz. The average simulated gain within the universal UHF RFID band was approximately 6.33 dBic.

a)

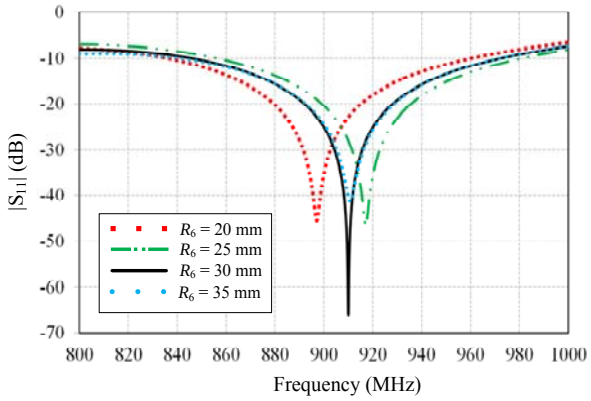

b)

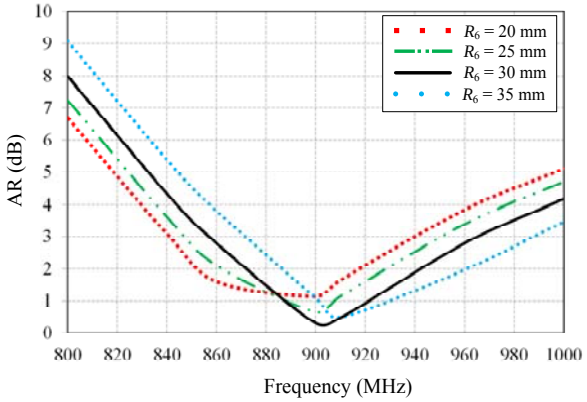

c)

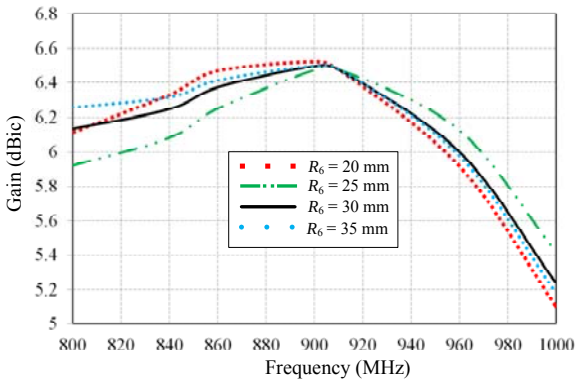

Fig. 7. The simulation results by varying R_6 (proposed antenna): (a) $|S_{11}|$, (b) AR and (c) gain.

Simulation and experimental results

This section presents the comparisons between the simulation outcomes of the proposed antenna and the measured results of the prototype antenna. Fig. 8 illustrates the front, perspective and cross-sectional views of the prototype antenna. Both the simulation and measured results relative to frequency encompass the $|S_{11}|$ BWs, the 3-dB AR BWs, the gains and the radiation patterns in the *x-y* and *x-z* planes. The comparison revealed a close resemblance between the simulation and the measurements, as shown in Figs. 9–11.

a)

b)

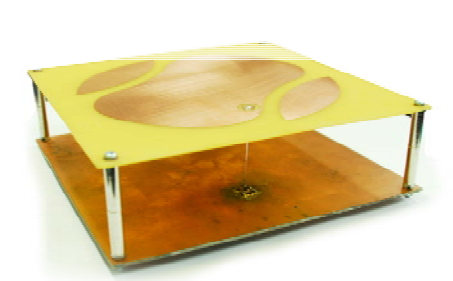

c)

Fig. 8. The proposed CP reader antenna for the universal UHF RFID band: (a) front view, (b) perspective view, (c) cross-sectional view.

The measurements were carried out using Agilent 8720 vector network analyzer. In Fig. 9 (a), the simulated and measured $|S_{11}|$ were resonant at the frequency of 910 and 902.6 MHz, with the $|S_{11}|$ BW of 13.89% (845.8-972.2 MHz) and 14.13% (837.6-966.2 MHz), respectively. The measured antenna gain, AR and radiation patterns are performed in the receiving mode in an anechoic chamber. The measurement setup uses transmitting standard dipole antenna with Anritsu MP-651B and the proposed antennas were separated by a distance of the far-field region. Mean-while, the boresight gain was measured based on the Friis transmission formula that can be accomplished by swept frequency. The simulated and measured AR at 860, 910 and 960 MHz of 2.79, 0.49 and 2.79 dB; and 2.54, 0.82 and 2.91 dB, respectively, while the simulated and measured 3-dB AR BW were 12.31% (853-965 MHz) and 12.41% (850.6-963.5 MHz), as shown in Fig 9 (b).

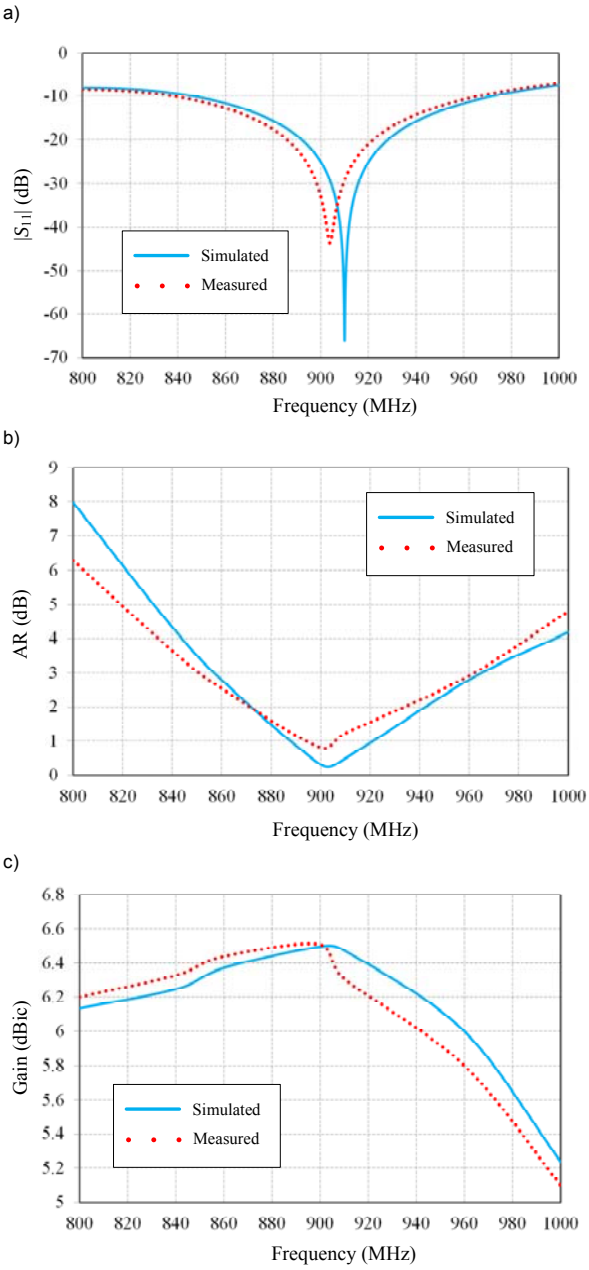

Fig. 9. The simulation and measurement results: (a) $|S_{11}|$, (b) AR, (c) gain.

Figure 9 (c) shows the simulated and measured gains at the frequencies of 860, 910 and 960 MHz of 6.37, 6.48 and 6.00 dBic; and 6.44, 6.31 and 5.8 dBic, respectively. The average simulated and measured gains within the universal UHF RFID band were, respectively, 6.28 and 6.18 dBic. Figure 10 illustrates the simulated and measured radiation patterns at 860, 910 and 960 MHz in the *x-z* plane. The simulated half-power beamwidths (HPBWs) of the co-polarization (left-hand circular polarization: LHCP) at 860, 910 and 960 MHz were 85.1°, 83.8° and 82.5°, respectively. The simulated cross-polarization (right-hand circular polarization: RHCP) levels at 860, 910 and 960 MHz at the main lobe of the radiation pattern were -16.1, -40 and -16.3 dB, respectively. The measured HPBWs of the co-polarization (LHCP) in the *x-z* plane at 860, 910 and 960 MHz were 84.1°, 83.6° and 82.5°, while the measured cross-polarization (RHCP) levels at 860, 910 and 960 MHz were -15.15, -40.00 and -15.45 dB, respectively.

Figure 11 depicts the simulated and measured radiation patterns at 860, 910 and 960 MHz in the *x-y* plane. The simulated half-power beamwidths (HPBWs) of the co-polarization (left-hand circular polarization: LHCP) at 860, 910 and 960 MHz were 84.4°, 83.7° and 82.5°, respectively. The simulated cross-polarization (right-hand circular polarization: RHCP) levels at 860, 910 and 960 MHz at the main lobe of the radiation pattern were -16.11, -37.11 and -16.11 dB, respectively. The measured HPBWs of the co-polarization (LHCP) in the *x-y* plane at 860, 910 and 960 MHz were 84°, 83.5° and 82.5°, while the measured cross-polarization (RHCP) levels at 860, 910 and 960.00 MHz were-16, -30 and -16.2 dB, respectively.

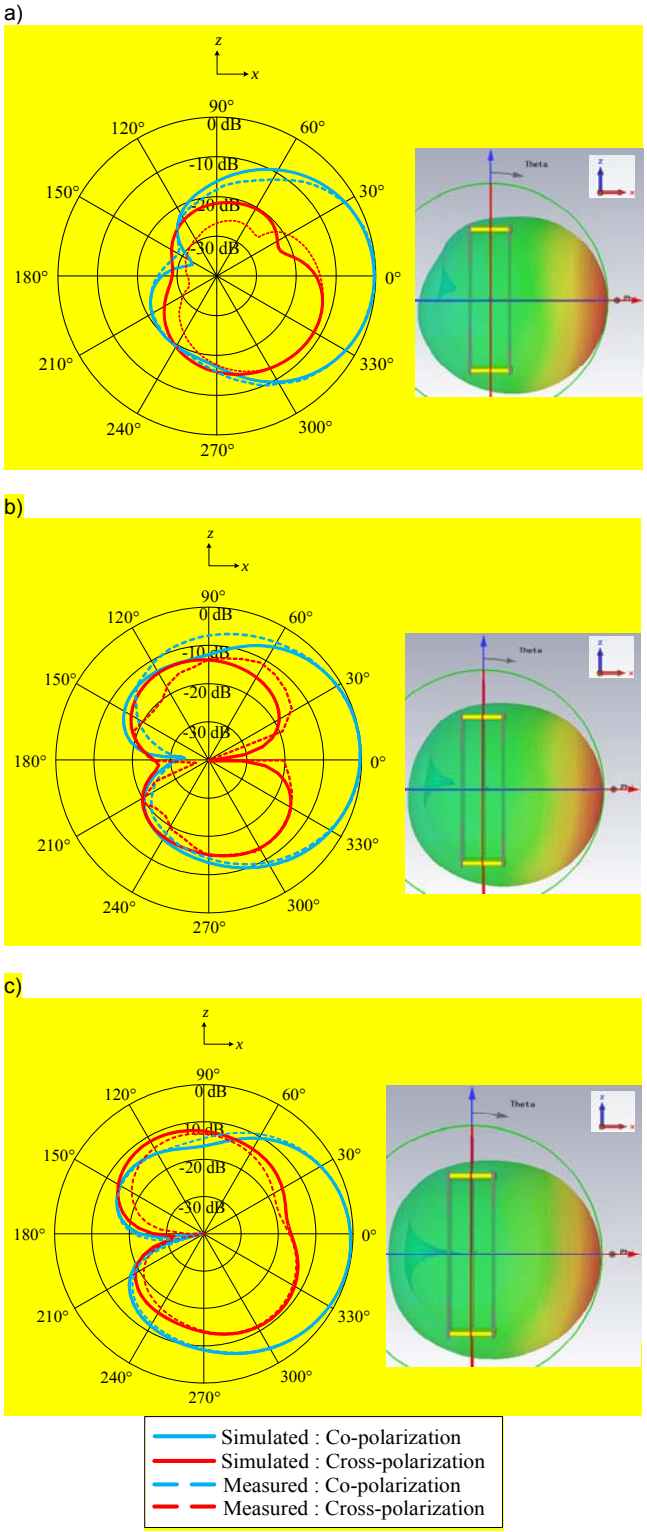

Fig. 10. The simulated and measured radiation patterns in the *x-z* plane (a) 860 MHz (b) 910 MHz and (c) 960 MHz

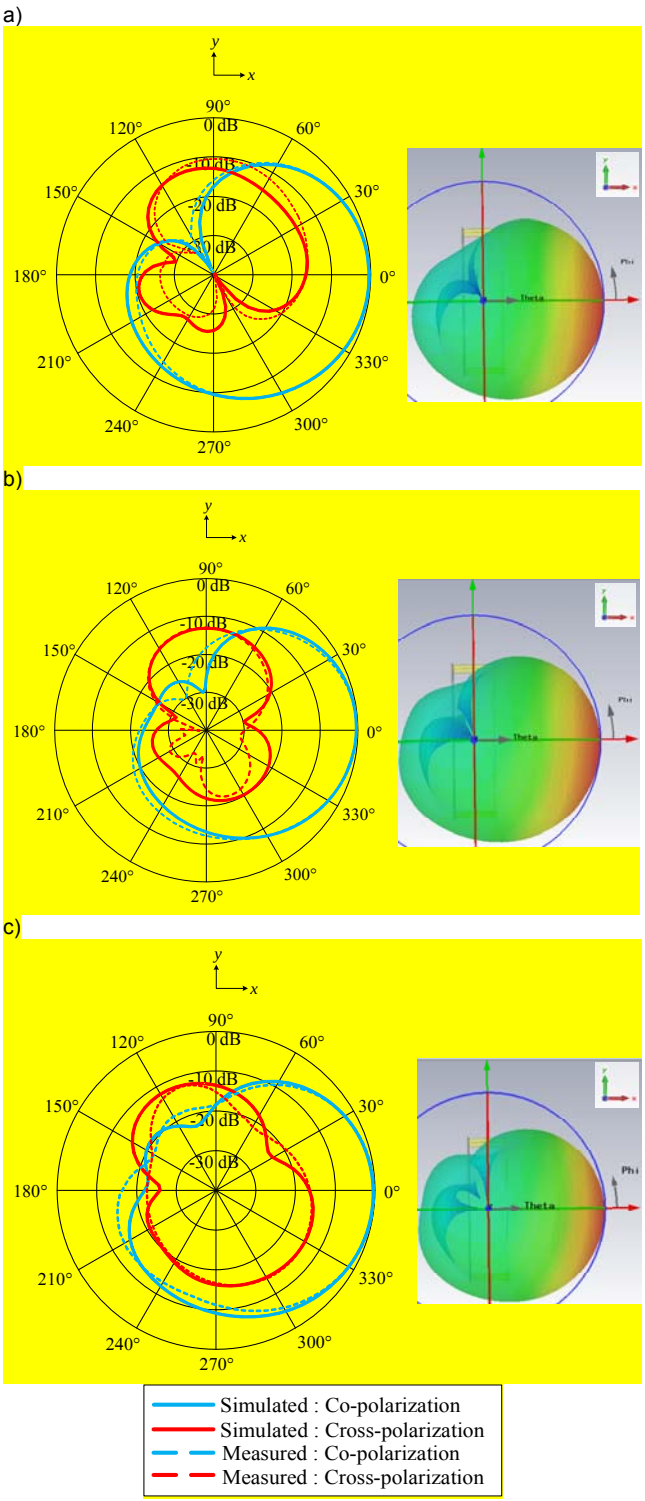

Fig. 11. The simulated and measured radiation patterns in the *x-y* plane (a) 860 MHz (b) 910 MHz and (c) 960 MHz

Conclusion

This research has proposed the tennis ball-shaped radiating plate integrated into the suspended-structure antenna for generating the CP and unidirectional radiations that cover the universal UHF RFID band. The proposed antenna was of simple design and 165×165×42 mm in dimensions. The experiments provided the relatively satisfactory results with regard to $|S_{11}|$ BW and 3-dB AR BW with the average gain of >6 dBic. The HPBWs of co-polarization (LHCP) in the *x-y* and *x-z* planes were >80°. Nevertheless, one shortcoming of the proposed antenna was the cross-polarization (RHCP) of >-20 dB at 860 and 960 MHz in both planes.

Acknowledgements

This work has been supported by the Thailand Research Fund (TRF) and the Thailand Science Research and Innovation (TSRI) through the Research Grant for New Scholar Program under Grant no. MRG6080070. The authors acknowledge with gratefulness the resources provided by the Institute of Research and Development (IRD), Rajamangala University of Technology Rattanakosin.

Authors: *Komkris Boonying, Department of Telecommunication Engineering, Faculty of Engineering, Rajamangala University of Technology Rattanakosin, Phutthamonthon, Nakhon Pathom, 73170, Thailand, E-mail: komkris.boo@rmutr.ac.th; Chuwong Phongcharoenpanich, Department of Telecommunication Engineering, Faculty of Engineering, King Mongkut's Institute of Technology Ladkrabang, BangKok, 10250, Thailand. E-mail: pchuwong@gmail.com.*

REFERENCES

[1] Finkenzeller K., *RFID Handbook: Fundamentals and Applications in Contactless Smart cards, Radio Frequency Identification and Near-Field Communication*, John Wiley & Sons Ltd., 2010.

[2] Curty P., Declercq M., Dehollain C., Joehl N., *Design and Optimization of Passive UHF RFID System*, Springer Science+Business Media, 2007.

[3] Aguirre J. I., *EPC global: A Universal Standard*, Available: http://web.mit.edu/smadnick/www/wp/ 2007-01.pdf. Feb., 2007

[4] Kumar G., Ray K. P., *Broadband Microstrip Antenna*, Artech House Inc., 2003.

[5] Bhartia P., Bahl I., Garg R., Ittipiboon A., *Microstrip Antenna Design Hand book*, Artech House, Inc., 2001.

[6] Balanis C.A., *Antenna Theory: Analysis and Design*, Wiley, Hoboken, NJ, 3rd., 2005.

[7] Wong K. L., *Compact and Broadband Microstrip Antenna*, New York, John Wiley & Sons, Inc., 2014.

[8] Lee J. M., Kim N. S., Pyo C. S., A circular polarized metallic patch antenna for RFID reader, *Asia-Pacific Conference on Communications*, (2005), 116-118.

[9] Chen Z. N., Chia M. Y. W., Broadband suspended plate antenna with probe-fed strip, *IEE proceeding Microwaves, Antennas and Propagation,* vol. 148 *(2001),* 37-40.

[10] Laohapensaeng T., and Boonying K., Dual-polarized microstrip antenna with high isolation using an inserted slot, *International Symposium on Intelligent Signal Processing and Communications Systems*, (2011), 1-5.

[11] Phongcharoenpanich Ch., Boonying K., Kosulvit S., Dual-polarized flat rectenna for 2.45 GHz, *IEEE-APS Topical conference on Antennas and Propagation in Wireless communications*, (2013), 1433-1436.

[12] Boonying K., Phongcharoenpanich Ch., Kosulvit S., Polarization reconfigurable suspended antenna using RF switches and P-I-N diodes, The 4th *Joint International conference on Information and Communication Technology, Electronic and Electrical Engineering*, (2014), pp. 5-8.

[13] Granholm J., Woelders K., Dual polarization stacked microstrip patch antenna array with very low cross-polarization, *IEEE Transactions on Antennas and propagation*, vol. 49 (2001), 1393-1402.

[14] Waterhouse R. B., Design of probe-fed stacked patches, *IEEE Transactions on Antennas and*

Propagation, vol. 47 (1999), 1767-1771.
[15]Mak C. L., Luk K. M., Lee K. F., Chow Y. L., Experimental study of a microstrip patch antenna with an L-shaped probe, *IEEE Transactions on Antennas and Propagation*, vol. 48 (2000), 777-783.
[16]Sim C. Y. D., Chi C. J., A slot loaded circularly polarized patch antenna for UHF RFID reader, *IEEE Transactions on Antennas and Propagation*, vol. 60 (2012), 4516-4521.
[17]Ooi B. L., Lee C. L, Kooi P. S., Chew S. T., A novel F-probe fed broadband patch antenna, *IEEE Antennas and Propagation Society International Symposium, (2001),* 73-76.
[18]Lu J. H., Wang S. F., Planar broadband circularly polarized antenna with square slot for UHF RFID reader, *IEEE Transactions on Antennas and Propagation*, vol. 61 (2013), 45-52.
[19]Mak C. L., Lee K. F., Luk K. M., Broadband patch antenna with T-shape probe, *IEE Proceedings Microwaves, Antennas and Propagation*, vol. 147 (2000), 73-76.
[20]Yang X. H., Shafai Y. L., Characteristics of aperture coupled microstrip antennas with various radiating patches and coupling apertures, *IEEE Transactions on Antennas and Propagation*, vol. 43 (1995), 72-78.
[21]Lee J. -K., Ahn Ch. H., Chang K., Broadband circularly polarized aperture-coupled microstrip antenna with dual-offset feedlines, *IEEE International Symposium on Antennas and Propagation*, (2011), 1127-1130.
[22]Wang Z., Fang S., Fu S., Jia S., Single-fed broadband circularly polarized stacked patch antenna with horizontally meandered strip for universal UHF RFID applications, *IEEE Transactions on Microwave Theory and Techniques*, vol. 59 (2011), 1066-1073.
[23]Kasabegoudar V. G., Vinoy K. J., Coplanar capacitively coupled probe fed microstrip antenna for wideband applications, *IEEE Transactions on Antennas and Propagation*, vol. 58 (2010), 3131-3138.
[24]Ridgers M. G., Odendaal J. W., Joubert J., Single-layer capacitive feed for wideband probe-fed microstrip antenna elements, *IEEE Transactions on Antennas and Propagation*, vol. 51 (2003), 1405-1407.
[25]Son H. W., Design of dual-polarised microstrip antenna with high isolation using capacitive feed, *Electronics Letters,* vol. 45 (2009), 383-385.
[26]Chen Z. N., Qing X., Chung H. L., A universal UHF RFID reader antenna, *IEEE Transactions on Microwave Theory and Techniques,* vol. 57 (2009), 1275-1282.
[27]Nasimuddin, Chen Z. N., Qing X., Asymmetric-circular shaped slotted microstrip antennas for circular polarization and RFID applications, *IEEE Transactions on Antennas and Propagation,* vol. 58 (2010), 3821-3828.
[28]Agarwal K., Nasimuddin, and Alphones A., RIS-base compact circularly polarized microstrip antennas, *IEEE Transactions on Antennas and Propagation*, vol. 61 (2013), 547-554.
[29]Nasimuddin, Qing X., Chen Z. N., Compact asymmetric-slit microstrip antennas for circular polarization, *IEEE Transactions on Antennas and Propagation,* vol. 59 (2011), 285-288.
[30]Lu J. H., Yu H. Ch., Wong K. L., Compact circular polarisation design for equilateral-triangular microstrip antenna with spur lines, *Electronics Letters*, vol. 34 (1998),1989-1990.
[31]Lin Y. F., Wang Y. K., Chen H. M., Yang Z. Z., Circularly polarized crossed dipole antenna with phase delay lines for RFID handheld reader, *IEEE Transactions on Antennas and Propagation*, vol. 60 (2012), 1221-1227.
[32]Lin Y. F., Chen H. M., Chu F. H., Pan S. C., Bidirectional radiated circularly polarised square-ring antenna for portable RFID reader, *Electronics Letters*, vol. 44 (2009), 1275-1282.
[33]Guha D., Resonant frequency of circular microstrip antennas with and without air gaps, *IEEE Transactions on Antennas and Propagation*, vol. 49 (2001), 55-59.